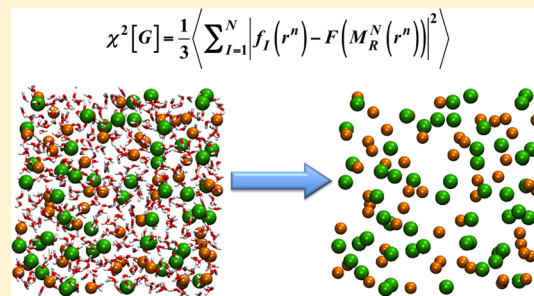


Solvent Free Ionic Solution Models from Multiscale Coarse-Graining

Zhen Cao, James F. Dama, Lanyuan Lu, and Gregory A. Voth*

Department of Chemistry, James Franck Institute, Institute for Biophysical Dynamics, and Computation Institute, University of Chicago, 5735 S Ellis Ave., Chicago, Illinois 60637, United States

ABSTRACT: Solvent free models for aqueous ionic solutions are derived using the multiscale coarse-graining (MS-CG) method to obtain many-body potentials of mean force and generalized Langevin equations to propagate the model in time. The resulting models are compared to other implicit solvent models for aqueous NaCl in terms of both sampling efficiency and accuracy. First, the equilibrium structural properties of the models are compared, and then the temperature dependence of the interior potentials of mean force are determined to obtain the pairwise entropy associated with the effective ionic interactions. After validating the equilibrium behavior of the new models, the dynamical properties are investigated using generalized Langevin equation dynamics simulations. The dynamical properties can be put into better agreement with the original atomistic models by introducing an exponential memory kernel to account for the strong coupling between the ions and their water solvation shells.



1. INTRODUCTION

The computer simulation of ionic solutions provides important insight into the physical principles underlying the properties of these ubiquitous systems. Classical atomistic force fields^{1–9} have been developed for these simulations and have been used to explore real systems in biology and materials science. Studies of this kind have obtained important results, for instance for ion pumps,^{10–13} DNA/RNA,^{14,15} and electrolytes.^{16,17} The distribution of ions in solution and the interactions between ions and proteins are critical in explanations of the behavior of the large biological systems.^{18,19} Additionally, simple ionic solutions are good prototypical systems for studying the structure–property relationships crucial for the design of complex electrolytes for specific applications.²⁰

At present, the bottleneck for molecular dynamics (MD) computer simulations used to calculate equilibrium ensemble average properties is the cost of sampling many uncorrelated structures. This is particularly true for complex biological processes, whose correlation time scales are well beyond the accessible time scales of most atomistic simulation methods. Therefore, it is useful to consider simpler, more efficient models for which statistically meaningful sampling is practically obtainable. Several methods for simplifying models of ionic solutions have been derived based on different assumptions, and aqueous ionic solutions such as NaCl at different concentrations are a typical benchmark used to evaluate these methods. One example is the concentration-dependent dielectric implicit solvent (CDDIS) modeling method,^{21,22} which fits many-body solvent-mediated effects into a concentration-dependent dielectric constant, based on the idea that different concentrations of ions inhibit the reorientation of water molecules to varying extents.²³ However, the first class of method requires calculating the potential of mean force (PMF) at infinite dilution for each type of ion–ion

pair using the constrained distance method, making the fitting process computationally intensive. Also, even after this simplification, the models mentioned above still contain long-range electrostatic interactions that may account for more than 40% of the total computational time in the atomistic MD model, thus limiting the potential speedup associated with using a simpler model. As an alternative to the method, DeMille and Molinero²⁴ iteratively fitted the angular distribution of the ions and waters using Stillinger–Weber three-body interactions and eliminated the long-range interaction. Unfortunately, they did not obtain a good radial distribution of the ions in water for high- and low-concentration solutions. There is therefore still much room to improve this type of model in the pursuit of increased efficiency and accuracy. It is also desirable to show how these models can provide more than equilibrium structural information, for instance dynamic correlations and thermodynamic transferability.

As an alternative to the implicit solvent models discussed above, this article will present a solvent-free coarse-grained (SFCG) modeling approach and investigate its behavior for NaCl solutions at varying concentrations. The SFCG method is an application of the multiscale coarse-graining (MS-CG) method^{25–29} to integrate out all solvent interactions,^{30,31} as well as long-range electrostatic interactions,^{32,33} into short-ranged effective pairwise interactions between ions. As this article will show, this method significantly improves over the CDDIS method in terms of both the calculation efficiency and the accuracy of the resulting models. In terms of pair radial distribution functions, the improvement is similar to that seen for inverse Monte Carlo³⁴ and molecular renormalization group

Received: August 20, 2012

Published: November 14, 2012

coarse-graining³⁵ methods applied to similar systems. The MS-CG method, however, matches both pair and many body correlations simultaneously through a generalized YBG hierarchy equation, making it more suited to reproducing many body correlations than those methods.^{36,37} This paper also evaluates the dynamical and thermodynamic properties of ionic solution models derived using the SFCG method, properties which have not been addressed in previous studies of similar methods applied to similar systems.^{34,35}

The remaining sections of this article are organized as follows: The methodology will be described in section II, where the theoretical background and practical implementation of the SFCG method will be presented. A detailed evaluation of this method applied to NaCl solution is provided in section III, including a comparison of structural properties between the SFCG model, the atomistic model, and the CDDIS model and a comparison of the dynamical properties between the SFCG model and the atomistic model. Generalized Langevin equations are also applied to improve the dynamical properties of the system. At the end of this section, the SFCG pair potentials are decomposed into their entropic and enthalpic contributions to investigate the thermodynamic driving forces in the system. The conclusions in section IV summarize the merits of the SFCG method and propose applications for future studies.

2. METHODOLOGY

2.1. Multiscale Coarse-Grained (MS-CG) Method and Solvent-Free Models. The MS-CG method initially proposed by Izvekov and Voth^{25,26} has been extended to a theoretical framework for systematically developing lower-resolution models from higher-resolution models to study the higher-resolution models' key characteristics with lower computational cost. This extended framework includes a thermodynamic bridge²⁷ between different models, different mapping strategies^{28,38} used to construct the coarse-grained (CG) model, and further theories based on closely related variational principles.^{39,40}

An MS-CG model employs an effective potential constructed from the atomistic trajectory using a variational force-matching method.²⁹ This method can be described in brief as choosing the force field that minimizes the MS-CG residual:

$$\chi^2[G] = \frac{1}{3N} \left\langle \sum_{I=1}^N |f_I(r^n) - F_I(M_R^N(r^n))|^2 \right\rangle \quad (1)$$

where $M_R^N(r^n)$ is a linear mapping operator to map atomistic particle configurations r^n onto CG particle configurations R^N , $F_I(M_R^N(r^n)) = -\partial/\partial R_I W(R^N)$ is the effective force on a single site I used in the CG force field, $f_I(r^n)$ is the atomistic force mapped onto CG particle I , and the expectation is taken with respect to a set of configurations sampled from the atomistic model in the canonical ensemble.

The SFCG model for the NaCl solution is constructed using this method and a mapping operator that does not incorporate any contribution from solvent degrees of freedom into the CG model. The SFCG force field minimizes the MS-CG residual over a large number of configurations, thus matching the forces obtained from atomistic simulation in the least-squares sense. The effective force between ions within a distance rarely sampled by atomistic simulations is obtained from the linear interpolation. The final result is a set of short-range tabulated forces that rigorously incorporate averaged long-range

Coulomb interactions and many-body solvent-mediated effects. In principle, the method is capable of producing efficient and precise models that can reproduce the key solute-specific properties of an atomistic solution model.

2.2. Concentration-Dependent Dielectric Implicit Solvent Model. A detailed description of the CDDIS method may be found in Shen et al.'s paper.²² These authors assume that an approximate free energy surface of the system may be expressed as a sum of pair potentials, each with the form:

$$V_p = \begin{cases} \int_{r_m}^r ds \left[\langle f_c \rangle_s + \frac{2k_B T}{s} \right] + \frac{q_1 q_2}{4\pi\epsilon_0\epsilon_E(c)r_m} & r < r_m \\ \frac{q_1 q_2}{4\pi\epsilon_0\epsilon_E(c)r_m} & r \geq r_m \end{cases} \quad (2)$$

where f_c is the force to constrain the ions, $\int_{r_m}^r ds [\langle f_c \rangle_s + 2k_B T/s]$ is the free energy normalized by eliminating the distance dependent entropy, and $\epsilon_E(c)$ is the concentration-dependent dielectric constant. The authors assume that the rotational motion of water molecules is suppressed by the high electrostatic field gradients in higher concentration solution and that this effect can be captured by varying the effective long-ranged dielectric constant with ion concentration; the particular values of the dielectric constant over a range of concentrations can be fit from the fluctuation of the dipole moment of the whole system in atomistic simulations over the desired range of concentrations.⁴¹

2.3. Simulation Setup. Atomistic models for aqueous NaCl solutions at five concentrations from 1 to 5 M were built up using Joung and Cheatham's NaCl model² and SPC/E water.⁴² Each system was equilibrated in the constant NPT ensemble at 300 K, 1 atm for 5 ns, with the average volume of the last 2 ns of simulation used to determine the volume of the solutions for constant NVT simulation. Next, the solutions were equilibrated in the NVT ensemble for 1 ns, and finally they were run for over 20 ns with a 2 fs time step, sampling the instantaneous coordinates and forces of the atoms every 200 fs. The effective forces between ions for the SFCG model were then constructed by minimizing the residual defined in eq 1, and the readers are referred to ref 29 for detailed description about the algorithm and MS-CG basis set used for this model.

These effective tabulated pair potentials between ions are shown in Figure 1 as a function of ionic concentration. These potentials were then employed for SFCG simulations of the ions. The initial positions of the ions in these simulations were obtained from the last frame of the atomistic simulation. Next, each was simulated in the constant NVT ensemble at 300 K for 22 ns with a 2 fs time step, sampling ion positions for analysis every 200 fs over the course of the last 20 ns. The SFCG model for a 1 M solution ran approximately 1200 times faster per nanosecond of simulation than the corresponding atomistic model, while the SFCG model for a 5 M solution was approximately 40 times faster than the corresponding atomistic model.

Next, an implicit solvent model was constructed and simulated using the CDDIS method of Shen et al.²² Potentials of mean force between pairs of ions at an infinite dilution were obtained using a constrained distance method. To carry out the constrained distance method, a series of independent simulations for each type of pair of ions at fixed separation in water was performed for separation distance values of every 0.2 Å between 2.0 Å and 12.0 Å, inclusive. Each simulation was

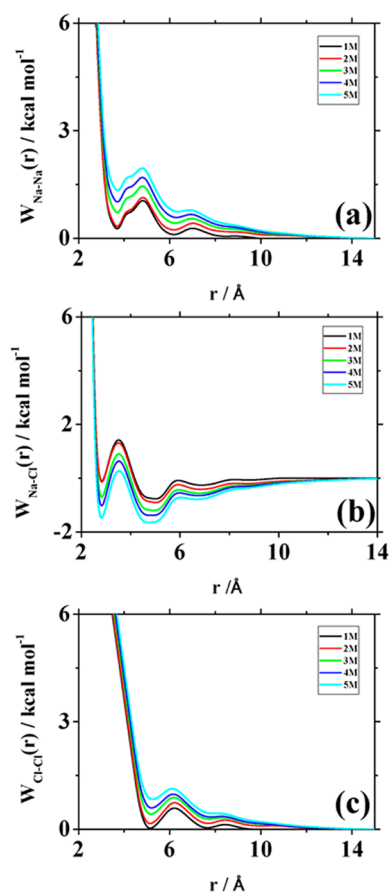


Figure 1. Effective interaction potentials from variational force matching for the ion pairs Na^+-Na^+ (a), Na^+-Cl^- (b), and Cl^--Cl^- (c) in 1 M (black), 2 M (red), 3 M (green), 4 M (blue), and 5 M (light blue) solutions.

performed for at least 5 ns; some with a separation distance shorter than 3 Å required over 10 ns of simulation to obtain a converged mean force. The interaction energy was obtained by integrating the force for each pair type over the distance from 12.0 Å, starting from $q_1q_2/4\pi\epsilon_0\epsilon_E(c)r_m$ at $r_m = 12.0$ Å, and each resulting interaction energy was then separated into a short-ranged interaction and a Coulomb interaction as follows:

$$V_p = V_{\text{short}} + \frac{q_1q_2}{4\pi\epsilon_0\epsilon_E(c)r} \quad (3)$$

3. RESULTS AND DISCUSSION

3.1. Structural Properties. The spatial distribution of the ions in solution is a key property when evaluating the quality of any ionic solution model, due to its crucial importance for predicting a number of macroscopic properties. In this paper, we focus primarily on the ion–ion radial distribution functions (RDFs). We computed RDFs for each different type of ion pair (Na^+-Na^+ , Na^+-Cl^- , and Cl^--Cl^-) in solution; the results for the atomistic model and SFCG model are shown in Figure 2a–i. The heights of the first peaks in the RDFs for each individual ion pair from each simulation at a given concentration are comparable to each other, indicating that the NaCl solutions are homogeneous in all concentrations studied herein and that the ions are well-hydrated by water molecules. This first peak corresponds to direct contact between the ions, which is well described by the force field used because it correctly fits the hydration energy of the ions in aqueous solution.^{43,44} On the other hand, the RDF for Na–Cl in ref 22 has a very high first peak, while the first peaks for Na–Na and Cl–Cl RDFs are relatively low. This indicates the direct contact between Na and Cl ions has a high probability, and NaCl may form ion pairs even at a relatively low concentration, e.g., 0.5 M solution. This may happen because the KBFF force field was fit to macroscopic properties,⁴⁵ e.g., activity coefficients, density,

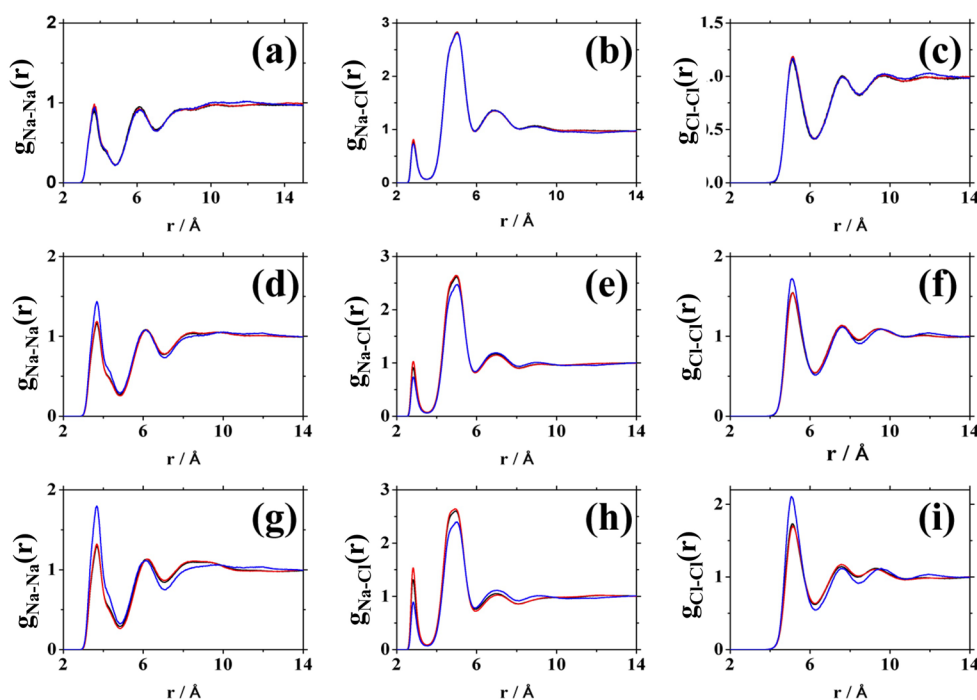


Figure 2. Radial distribution functions of the atomistic models (black), SFCG models (red), and concentration-dependent dielectric implicit solvent models (blue) in 1 M (a–c), 3 M (d–f), and 5 M (g–i) solutions.

and compressibility, while it is deficient in the description of the detailed solution structure. If the optimal SFCG force field found using the variational force-matching method accurately reproduces the PMF of the solution, the SFCG models will reproduce the structural correlations between ions accurately, and the heights of the peaks in the RDFs for the SFCG model will show good agreement with the behavior in the all-atom model. In fact, we do see that the concentration-dependent RDFs of the atomistic ionic solution models are well-reproduced by the SFCG models, and that the SFCG method works almost equally well in all of the various ionic solutions tested.

To provide a comparison between the SFCG models and other implicit solvent models for ionic solutions, simulations using the CDDIS model were also performed as a benchmark. The system was set up following the instructions of Shen et al.²² for the most part but employing Cheatham's force field in the underlying atomistic models for better comparison to the SFCG models. In summary, the CDDIS method employs the effective potential from solutions at infinite dilution for the short ranged noncoulomb interaction, assuming this is constant with respect to changes in concentration, while the long-ranged part of the potential is fit using a concentration dependent dielectric constant, giving the model more transferability. In contrast, the SFCG method uses a linear least-squares algorithm to minimize the mismatch in forces between the atomistic and CG models at each concentration to find optimized potentials for different concentration solutions, that is, tabulated many body pairwise decomposable potentials of mean force for the models at each concentration. The RDFs for each ion pair type in 1 M, 3 M, and 5 M solutions using atomistic, SFCG, and CDDIS models are shown in Figure 2. In 1 M solutions, both the SFCG model and the CDDIS model reproduce the atomistic simulation results very well. As ion concentration increases, the accuracy of the CDDIS model decreases, as observed in previous studies.^{21,22} However, the SFCG model still works very well even in the 5 M solutions, as expected from previous applications of systematic CG methods to ionic solution.³⁴

As ion concentration increases, the probability that a given ion is simultaneously in contact with multiple other ions increases significantly. To correctly describe such a structure, the effective interaction between the ions must include the effects of many-body interactions. These effects are incorporated in the CDDIS model through a concentration-dependent dielectric constant, based on the understanding that ions pin the orientation of nearby water molecules, thereby decreasing the polarizability of the solvent. In the force-matching method, these effects are decomposed into pairwise interactions between ions based on an approximate, discretized Yvon–Born–Green (YBG) equation.³⁶ Because force matching incorporates many-body effects in this systematic way, the SFCG models present better radial distribution functions compared with the CDDIS models in concentrated solution.

To further explore the merits of the SFCG models, it is possible to compare the three-body correlations between ions in 5 M solutions. The three-body structures can be partially characterized by using the angular distribution function (ADF), which is defined as

$$P(\theta) = \frac{1}{W} \left\langle \sum_i \sum_{j \neq i} \sum_{k > j} \delta(\theta - \theta_{ijk}) \right\rangle \quad (4)$$

where W is a normalization constant and θ is the angle between the i th, j th, and k th ion hinged at the j th ion. The distance cutoff was chosen to be 6.0 Å to match the second minimum of the RDF between Na⁺ and Cl[−]. The results for the atomistic model, CDDIS model, and SFCG model of the 5 M solution are shown in Figure 3. It is clear that the SFCG model can

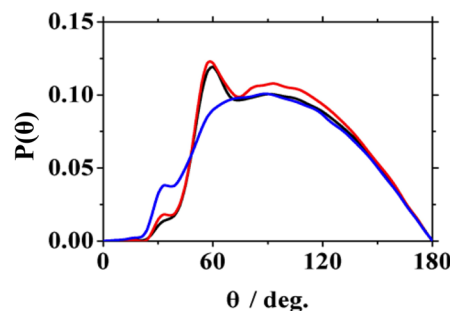


Figure 3. Angular distribution functions of the atomistic model (black), SFCG model (red), and concentration-dependent dielectric implicit solvent model (blue) of a 5 M solution.

reproduce the angular distribution of the ions in solution more accurately than the CDDIS model, which indicates that the SFCG model incorporates many-body correlations more thoroughly than the CDDIS model does.

3.2. Dynamical Properties. Several dynamical properties of the SFCG model were also evaluated⁴⁶ and compared with those of the atomistic MD model. To evaluate these properties, first the atomistic and SFCG models were resampled in the constant NVE ensemble for 100 ps, recording the force, velocity, and position of each ion in the simulation after every 2 fs time step, and then the velocity autocorrelation function (VACF) and its Fourier transform were calculated. The results are shown in Figure 4 for 5 M concentration. Although the SFCG model may correctly describe the equilibrium ion structure, the ions diffuse much faster than those in the atomistic model because certain dynamical effects from water molecules surrounding the ions, such as friction and caging, are not captured in the SFCG force field.

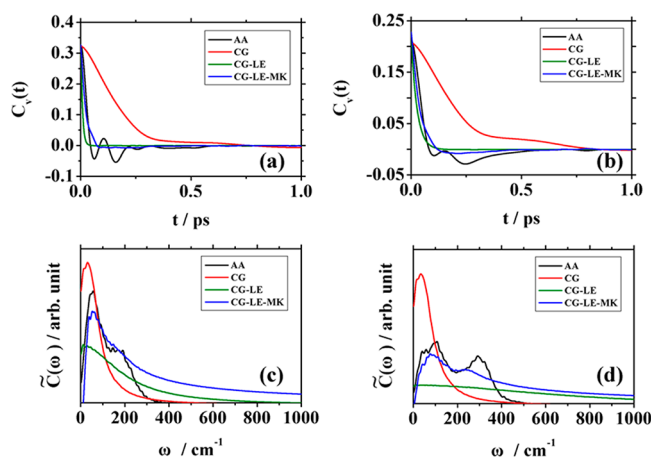


Figure 4. Velocity autocorrelation function (VACF) for (a) Na⁺ and (b) Cl[−] and Fourier transform of the VACF for (c) Na⁺ and (d) Cl[−] for the various models for 5 M ionic solution: atomistic (black lines), no noise SFCG (red lines), Markovian noise SFCG (blue lines), and exponentially correlated noise SFCG (green lines).

To improve the dynamical properties of the SFCG model, the force fluctuations and friction originating from the solvent molecules must be included implicitly in the model. To accomplish this, the equation of motion is cast as a generalized Langevin equation (GLE):

$$m\ddot{q} = F_{\text{eff}}[q(t)] - \int_0^t dt' \eta(t-t')\nu(t') + F_{\text{rand}}(t) \quad (5)$$

where F_{eff} is the effective force obtained by using the force-matching method to match the atomistic simulation.⁴⁷ This model was first tested using the Markovian assumption $\eta(t-t') = \eta(0) \times \delta(t-t') = -\tilde{C}_{\delta F}/3D$ with $\tilde{C}_{\delta F}$ being the Laplace transform of the autocorrelation function $\tilde{C}_{\delta F} = \langle \delta F(t) \cdot \tilde{\nu}(0) \rangle$, where $\delta F(t)$ is the instantaneous force difference between the atomistic force and the effective force. The friction coefficient for Na^+ is $\eta_{\text{Na}}/m_{\text{Na}} = 243 \text{ ps}^{-1}$, while for Cl^- it is $\eta_{\text{Cl}}/m_{\text{Cl}} = 73 \text{ ps}^{-1}$, both indicating that strong fluctuation terms must be added to the SFCG model, since by the fluctuation–dissipation theorem, $\langle F_s(t) \cdot F_s(0) \rangle = 6\eta_0 k_B T \delta(t)$. A more detailed description of the theoretical background and the practical implementation of this CG dynamical modeling strategy may be found in previous work.⁴⁷

The merit of this method is that it corrects the CG diffusion constant to match the diffusion constant of the atomistic simulation by including the fluctuation of the solvents as white noise. However, from the comparison in Figure 4, it is clear that this approach still does not describe the ion dynamics satisfactorily. In atomistic MD simulations, the water molecules form an ordered cage surrounding the central ion with a reordering time scale comparable to the inertial time scale of the ion, and the interactions between each ion and its cage result in a strong coupling between the solute and solvent molecules acting on frequencies comparable to the motion of individual ions. Hence, the Markovian approximation is not applicable to this type of system; the friction term should include the effect of the velocity for several previous steps. To address this, an exponential memory kernel is introduced:⁴⁸

$$\eta(t-t') = \gamma(0) \exp\left[-\frac{t-t'}{\tau}\right] \quad (6)$$

where $\gamma(0) = \beta \langle (\delta F)^2 \rangle / m$ is the friction constant which can be determined directly from the average force fluctuation acting on ions in the atomistic simulation trajectory, τ is the relaxation time obtained from $\tau = [\beta m D \gamma(0)]^{-1}$, and D is the diffusion constant from the integration of the VACFs. The friction term is obtained from a right Riemann sum integration of the memory kernel over the relaxation time discretized using the time step of the dynamics, and the time correlated random force is generated using the algorithm in Pollak and Berezhkovskii.⁴⁹ The dynamical properties of this model are also shown in Figure 4 (blue lines). These are much improved and reproduce almost all the information in the low-frequency space, although the short-time behavior (shorter than 0.3 ps) for the VACFs is still not well-reproduced. The dynamic properties for Cl^- are better reproduced compared with those for Na^+ cations. We hypothesize that this is mainly because the ionic radius of the Cl^- is larger than that of Na^+ , so the ionic charge is less concentrated, the solvation shell surrounding the Cl^- is less rigid, and the interaction between the anion and surrounding water molecules is not as strong.

3.3. Thermodynamic Quantities. On the basis of the fact that the effective force for each SFCG model is actually a

pairwise approximation to the many-ion potential of mean force from the atomistic system it represents, the many-dimensional integral of the effective many-body forces can be considered an approximate PMF.⁵⁰ This PMF, while decomposed into pair interactions, is not an approximation to the pair PMF obtained by taking the logarithm of the radial distribution function but rather to the pairwise potential that would be found precisely using the YBG hierarchy.³⁶ As an approximate PMF, it may be interpreted in terms of entropic and internal energetic contributions. To decompose these thermodynamic contributions to the effective force in the SFCG model, five simulations using the atomistic model were performed at 290 K, 300 K, 310 K, 320 K, and 330 K, respectively, and the entropy was obtained by using a finite difference approximation to the definition of the entropy in the canonical ensemble, $\Delta S = \Delta A(T_1) - \Delta A(T_2)/T_1 - T_2|_V$. Each of the simulations was performed as the original atomistic simulations were using the same parameters aside from the changed temperature, running for 22 ns, and sampling for only the last 20 ns.

The results of this thermodynamic decomposition of the effective ion–ion SFCG pair interactions are shown in Figure 5, where the wells of the enthalpy curves correspond to differing numbers of solvation shells between the two ions. It can be seen that the entropic and energetic interactions between the ions act counter to each other: when the ions are well-solvated by the surrounding water molecules, the system may benefit from an energetic effect but suffer from an entropy penalty due to local ordering. When such an ordered structure becomes looser, ions may gain in entropy while incurring an energetic penalty. Such behavior is seen in our results, in which the enthalpy peaks are always nearby the entropy wells and vice versa.

The behavior of the entropy and internal energy curves is different for the like ions and the counterions. This is because the force driving aggregation can be entropic for both hydrophobic particles^{51,52} and hydrophilic particles⁵³ in aqueous solution. Each ion is well-solvated by water molecules when it is at a large distance from other ions. The ordered solvation structure incurs an entropy penalty. As counterions approach one another, a portion of the solvation shell for each is broken, releasing water molecules into the aqueous solution as the counterions replace those water molecules. This is an entropy-driven process; although the ions incur an effective internal energy penalty due to lost water solvation, the entropy benefit from the released water molecules dominates, as can be seen in that the value of the green line in Figure 5b is quite negative when two counterions are close to each other. On the other hand, the changes as two like ions approach one another are very different. When two like ions are in close proximity, water molecules form a rigid structure between the two ions. Such structures incur a large entropy penalty that inhibits aggregation even though the effective energy of pair interaction is favorable due to the increased water solvation. The comparison between Figure 6a–c clearly shows examples where close pairs of like ions enhance the order of the water molecules around them relative to far pairs, while close pairs of counterions order the water around them less than far pairs. The driving forces of aggregation in aqueous solution thus appear to be well accounted for by the effective force used in the SFCG models.

We have also evaluated the temperature dependence of the pairwise approximation to the many body potential of mean force (PMF) obtained from the force matching method. The

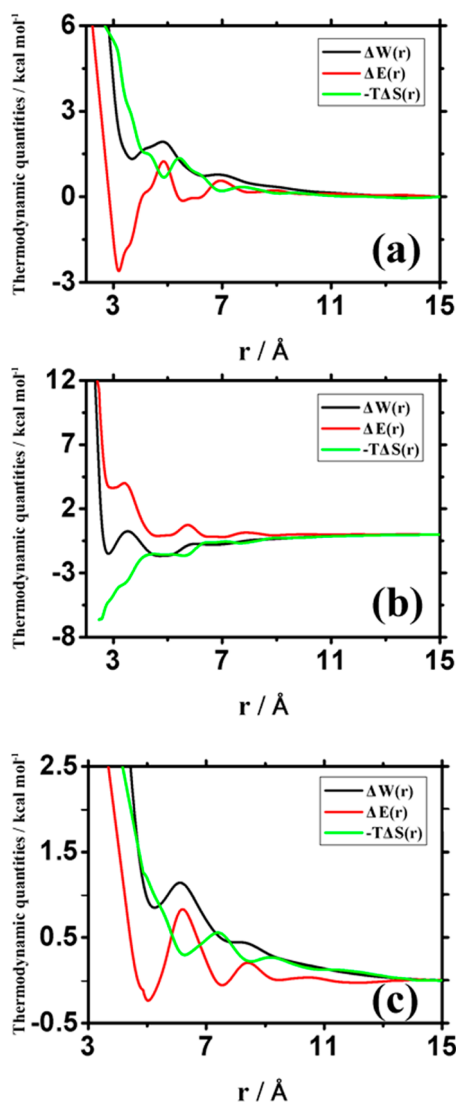


Figure 5. Pair thermodynamic quantities as a function of distance for the SFCG pairwise effective interactions for ion pairs $\text{Na}^+ - \text{Na}^+$ (a), $\text{Na}^+ - \text{Cl}^-$ (b), and $\text{Cl}^- - \text{Cl}^-$ (c) in solution obtained from the finite difference approximation to the entropy. Black lines represent pair Helmholtz free energies, red lines represent pair internal energies, and green lines represent pair entropies.

approximate PMFs obtained for the simulation at different temperatures are shown in Figure 7a, while the linear correlation for the first minima in the approximate PMF curve for different concentrations is presented in Figure 7b. This confirms that the pairwise interactions can be approximated as linear functions of temperature over the range from 290 to 330 K. The results indicate that the PMF in this area may be separated into a temperature independent potential energy and an entropic part proportional to temperature; the SFCG PMF at any temperature in this range can be obtained by using this transferable approximation to the free energy as in ref 50 for more general coarse-grained systems over a more limited temperature range.

4. CONCLUSIONS

This paper presents the properties of the SFCG method for aqueous ionic solution models and compares their structural properties with those of CDDIS models for NaCl solutions.

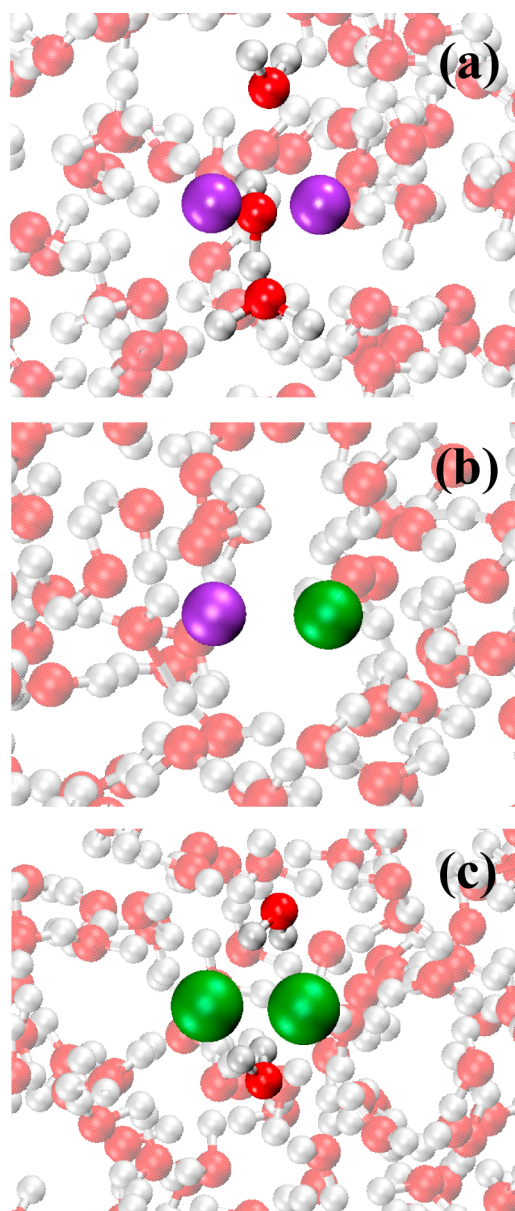


Figure 6. Snapshots of the solvation structure surrounding isolated pairs of nearby ions. When two Na^+ cations (a) or two Cl^- anions (c) are close to each other, several water molecules are highly ordered in the intermediate area between two ions, while when one Na^+ cation and one Cl^- anion are close to each other (b), the water molecules between these ions are released from the intermediate area.

The present work shows that the force-matching-based SFCG method is capable of integrating out the electrostatic interactions between ions into short-ranged effective potentials while also decomposing the many-body PMF into a sum of effective pairwise interactions. Our comparisons indicate that the force-matching-based SFCG method generates very accurate solvent-free models.

The dynamical properties of the SFCG ions can be improved by using a generalized Langevin equation (GLE) to match the diffusion constant from the atomistic simulation. The dynamical properties of the ions in solution are further improved by including a non-Markovian memory kernel in the GLE, becoming accurate for all but the shortest time scales.

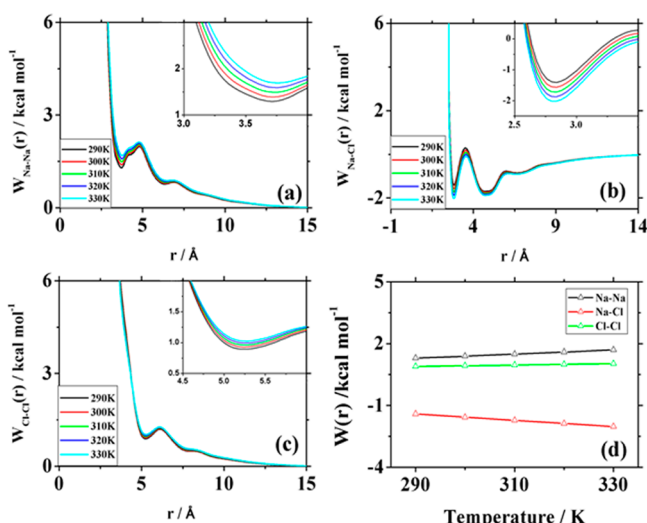


Figure 7. Temperature dependence of the effective interaction between the ions: the effective interaction for Na–Na (a), Na–Cl (b), Cl–Cl(c), and the linear correlation for the interaction at the first well (d).

The effective forces used in SFCG models are a close approximation to the true mean forces of the ionic system, and it is possible to obtain approximate entropy and internal energy surfaces of the system from these effective forces. In this paper, we show that the entropy and internal energy surfaces obtained from the effective ion force confirm that ion dissociation in solution can be an entropy-driven process, highlighting another advantage of the force-matched SFCG models as thermodynamically informative constructs.

AUTHOR INFORMATION

Corresponding Author

*Fax: 773-702-0805. Phone: 773-702-7250. E-mail: gavoth@uchicago.edu.

Notes

The authors declare no competing financial interest.

ACKNOWLEDGMENTS

This research was supported by the National Science Foundation (NSF grant CHE-1214087) and in part by a grant of computer time from the Department of Defense (DOD) High Performance Computing Modernization Program at the Army Research Laboratory DOD Supercomputing Resource Center.

REFERENCES

- (1) Gee, M. B.; Cox, N. R.; Jiao, Y.; Benteinitis, N.; Weerasinghe, S.; Smith, P. E. *J. Chem. Theory Comput.* **2011**, *7*, 1369.
- (2) Joung, I. S.; Cheatham, T. E., III. *J. Phys. Chem. B* **2008**, *112*, 9020.
- (3) Lamoureux, G.; Roux, B. *J. Phys. Chem. B* **2006**, *110*, 3308.
- (4) Jensen, K. P.; Jorgensen, W. L. *J. Chem. Theory Comput.* **2006**, *2*, 1499.
- (5) Wang, J. M.; Cieplak, P.; Kollman, P. A. *J. Comput. Chem.* **2000**, *21*, 1049.
- (6) Foloppe, N.; MacKerell, A. D. *J. Comput. Chem.* **2000**, *21*, 86.
- (7) Dang, L. X. *J. Am. Chem. Soc.* **1995**, *117*, 6954.
- (8) Smith, D. E.; Dang, L. X. *J. Chem. Phys.* **1994**, *100*, 3757.
- (9) Beglov, D.; Roux, B. *J. Chem. Phys.* **1994**, *100*, 9050.
- (10) Poulsen, H.; Khandelia, H.; Morth, J. P.; Bubltz, M.; Mouritsen, O. G.; Egebjerg, J.; Nissen, P. *Nature* **2010**, *467*, 99.

- (11) Ratheal, I. M.; Virgin, G. K.; Yu, H.; Roux, B.; Gatto, C.; Artigas, P. *Proc. Natl. Acad. Sci. U. S. A.* **2010**, *107*, 18718.
- (12) Yu, H.; Ratheal, I. M.; Artigas, P.; Roux, B. *Nat. Struct. Mol. Biol.* **2011**, *18*, 1159.
- (13) Yu, H.; Noskov, S. Y.; Roux, B. *Proc. Natl. Acad. Sci. U. S. A.* **2010**, *107*, 20329.
- (14) Pérez, A.; Luque, F. J.; Orozco, M. *Acc. Chem. Res.* **2012**, *45*, 196.
- (15) Swadling, J. B.; Coveney, P. V.; Greenwell, H. C. *J. Am. Chem. Soc.* **2010**, *132*, 13750.
- (16) Yang, L.; Huang, K. *J. Phys. Chem. B* **2010**, *114*, 8449.
- (17) Kalcher, I.; Dzubiella, J. *J. Chem. Phys.* **2009**, *130*, 134507.
- (18) Zhang, Y.; Cremer, P. S. *Proc. Natl. Acad. Sci. U. S. A.* **2009**, *106*, 15249.
- (19) dos Santos, A. P.; Levin, Y. *Phys. Rev. Lett.* **2011**, *106*, 167801.
- (20) Molina, J. J.; Dufreche, J.-F.; Salanne, M.; Bernard, O.; Jardat, M.; Turq, P. *Phys. Rev. E* **2009**, *80*, 065103.
- (21) Hess, B.; Holm, C.; van der Vegt, N. *Phys. Rev. Lett.* **2006**, *96*, 147801.
- (22) Shen, J.-W.; Li, C.; van der Vegt, N. F. A.; Peter, C. *J. Chem. Theory Comput.* **2011**, *7*, 1916.
- (23) Debye, V. P.; Hückel, E. *Phys. Z.* **1923**, *24*, 185.
- (24) DeMille, R. C.; Molinero, V. *J. Chem. Phys.* **2009**, *131*, 034107.
- (25) Izvekov, S.; Voth, G. A. *J. Phys. Chem. B* **2005**, *109*, 6573.
- (26) Izvekov, S.; Voth, G. A. *J. Chem. Phys.* **2005**, *123*, 134105.
- (27) Noid, W. G.; Chu, J.-W.; Ayton, G. S.; Krishna, V.; Izvekov, S.; Voth, G. A.; Das, A.; Andersen, H. C. *J. Chem. Phys.* **2008**, *128*, 244114.
- (28) Noid, W. G.; Liu, P.; Wang, Y.; Chu, J.-W.; Ayton, G. S.; Izvekov, S.; Andersen, H. C.; Voth, G. A. *J. Chem. Phys.* **2008**, *128*, 244115.
- (29) Lu, L.; Izvekov, S.; Das, A.; Andersen, H. C.; Voth, G. A. *J. Chem. Theory Comput.* **2010**, *6*, 954.
- (30) Izvekov, S.; Voth, G. A. *J. Phys. Chem. B* **2009**, *113*, 4443.
- (31) Lu, L.; Voth, G. A. *J. Phys. Chem. B* **2009**, *113*, 1501.
- (32) Izvekov, S.; Swanson, J. M. J.; Voth, G. A. *J. Phys. Chem. B* **2008**, *112*, 4711.
- (33) Shi, Q.; Liu, P.; Voth, G. A. *J. Phys. Chem. B* **2008**, *112*, 16230.
- (34) Lyubartsev, A. P.; Laaksonen, A. *Phys. Rev. E* **1997**, *55*, 5689.
- (35) Savelyev, A.; Papoian, G. A. *J. Phys. Chem. B* **2009**, *113*, 7785.
- (36) Noid, W. G.; Chu, J.-W.; Ayton, G. S.; Voth, G. A. *J. Phys. Chem. B* **2007**, *111*, 4116.
- (37) Mullinax, J.; Noid, W. G. *Phys. Rev. Lett.* **2009**, *103*, 198104.
- (38) Das, A.; Andersen, H. C. *J. Chem. Phys.* **2009**, *131*, 034102.
- (39) Krishna, V.; Noid, W. G.; Voth, G. A. *J. Chem. Phys.* **2009**, *131*, 024103.
- (40) Das, A.; Andersen, H. C. *J. Chem. Phys.* **2010**, *132*, 164106.
- (41) Neumann, M. *Mol. Phys.* **1983**, *50*, 841.
- (42) Berendsen, H. J. C.; Grigera, J. R.; Straatsma, T. P. *J. Phys. Chem.* **1987**, *91*, 6269.
- (43) Joung, I. S.; Cheatham, T. E., III. *J. Phys. Chem. B* **2008**, *112*, 9020.
- (44) Joung, I. S.; Cheatham, T. E., III. *J. Phys. Chem. B* **2009**, *113*, 13279.
- (45) Weerasinghe, S.; Smith, P. E. *J. Chem. Phys.* **2003**, *119*, 11342.
- (46) Berne, B. J.; Harp, G. D. *Adv. Chem. Phys.* **1970**, *17*, 63.
- (47) Izvekov, S.; Voth, G. A. *J. Chem. Phys.* **2006**, *125*, 151101.
- (48) Berne, B. J.; Boon, J. P.; Rice, S. A. *J. Chem. Phys.* **1966**, *45*, 1086.
- (49) Pollak, E.; Berezhkovskii, A. M. *J. Chem. Phys.* **1993**, *99*, 1344.
- (50) Lu, L.; Voth, G. A. *J. Chem. Phys.* **2011**, *134*, 224107.
- (51) Choudhury, N.; Pettitt, B. M. *J. Phys. Chem. B* **2006**, *110*, 8459.
- (52) Shimizu, S.; Chan, H. S. *J. Am. Chem. Soc.* **2001**, *123*, 2083.
- (53) Kovalenko, A.; Hirata, F. *J. Chem. Phys.* **2000**, *112*, 10403.